CFD Modeling of Thermoelectric Air Duct System for Cooling of Building Envelope.

by

Syaza Yasmin Bt Mohamad Yusoff

16031

Dissertation submitted in partial fulfilment of

the requirements for the

Bachelor of Engineering (Hons) (Mechanical)

JANUARY 2016

Universiti Teknologi PETRONAS

Bandar Seri Iskandar

31750 Tronoh

Perak Darul Ridzuan

CERTIFICATION OF APPROVAL

CFD Modeling of Thermoelectric Air Duct System for Cooling of Building Envelope.

by

Syaza Yasmin Bt Mohamad Yusoff
16031

A project dissertation submitted to the

Mechanical Engineering Programme

Universiti Teknologi PETRONAS

in partial fulfillment of the requirement for the

BACHELOR OF ENGINEERING (Hons)

(MECHANICAL ENGINEERING)

Approved by,

_____
(Khairul Habib)

UNIVERSITI TEKNOLOGI PETRONAS
TRONOH, PERAK
January 2016

CERTIFICATION OF ORIGINALITY

This is to certify that I am responsible for the work submitted in this project, that the original work is my own except as specified in the references and acknowledgements, and that the original work contained herein have not been undertaken or done by unspecified sources or persons.

_____

SYAZA YASMIN BT MOHAMAD YUSOFF

ACKNOWLEDGEMENT

In the name of Allah, the Most Gracious, the Most Merciful. Praise to Him the Almighty that in his will and given strength, the author managed to complete this final year project within the time required.

Many thanks to the supervisor, Dr. Khairul Habib, for his supervision, support, and advice not only in project matter but also for the future life and employment. With his guidance, the project can properly be done without a lot of problem.

The author would like to express gratitude to Kashif Irshad and Salman bin Kashif for their willingness in teaching all necessary knowledge, procedures and helped to understand more on the cooling system. These people are so kind and helped a lot in completing this report. Thanks to all fellow friends and everyone who have directly or indirectly lent a helping hand here and there. Not forgetting author's parents and family, who had always given support in completing this project.

May Allah bless and pay them all.

Contents

List of Figures

List of Tables

ABSTRACT

A multi-stage of thermoelectric modules is used in an air duct as a cooling system. The ThermoElectric Air Duct (TE-AD) system is installed with 24 ThermoElectric Modules (TEMs) installed with heat sink, cold plate and exhaust fan for air circulation. To simplify the TE-AD system, a three-dimensional model is proposed and implemented in a Computational Fluid Dynamics (CFD) simulation environment (FLUENT). An analysis of results, obtained in the experimental study of the TE-AD system for cooling of building envelope, shows that temperature gradient of 3.0-5.3°C between interior and the exterior of the building envelope was achieved. The current supplied to the TEMs are constant while the air flow rate is varied to investigate the factor on the performance of the thermoelectric. Using the TE-AD simulation model, it can be implemented to various CFD models of heat sources to predict the system performance for optimization.

CHAPTER 1

INTRODUCTION

1.1 Background of Study

As the world's population increases along with industrial revolution, energy demand for thermal comfort purpose continues to escalate. At the same time those in developed countries consume greatly more resources than those in developing nations, a situation which is inevitable but also unsustainable as populations increase and as developing nations aspire to the consumer lifestyle enjoyed in the West.

In conclusion, throughout the history, development in air conditioning is baffled to accomplish adequate thermal comfort within the building envelope. To overcome this high energy requirement, environmental concerns and the drive to reduce CO2 emissions from building have led to an increased interest in renewable energy as sources of cooling for buildings.

Numerical study are necessary when a detailed analysis of a thermoelectric air duct performance is required. The finite element method (FEM) has become an essential solution technique in many areas of engineering and physics. The FEM versatility lies in its ability to model arbitrary shaped structures, work with complex materials, and apply various types of loading and boundary conditions. The method can easily be adapted to different sets of constitutive equations, which makes it particularly attractive for coupled-physics simulation.In this work a finite element model was developed using tools probed enough to guarantee its reliability. Only a specific subroutine was designed and programmed in ANSYS Fluent.

The study of the behaviour of TE-AD is basically a problem of simultaneous thermal and electrical flows in a regular geometry. ANSYS, a commercial program of

finite element method, solves this type of problems with high accuracy as stated a lot of validated tests.

. This air-conditioning system, TE-AD (thermoelectric air duct) system use TEMs (thermoelectric modules) to lower the temperature of the airflow. This study aims to analyse energy efficiency of the TE-AD system for cooling of building envelope.

1.2 Problem Statement

Performance of the TE-AD system is directly affected by the ambient temperature and different flow velocity. In experimental study, the quantitative description of the flow distribution using measurement is limited to number of points, time, range of problems and operating conditions. The ANSYS finite element program has a large library of elements that support structural, thermal, fluid, acoustic, and electromagnetic analyses, as well as coupled-field elements that simulate the interaction between the above fields. Examples of ANSYS coupled-physics capabilities include thermal-structural, fluid-structure, electromagnetic-thermal, thermal-electric, structural-thermal-electric, piezoelectric, piezoresistive, magneto-structural, and electrostatic-structural analyses [1]. Using this features, TE-AD model can be adapted into the Ansys Fluent to generate a general 3-D finite element formulation that can be used to test for various boundary conditions.

1.3 Objective

In conjunction with above problem statement, the objective is to:

1 To study all temperature dependent characteristics of the TE-AD using ANSYS CFD-Fluent simulation.
2 To validate the CFD computation result with experimental result.

1.4 Scope of Study

The main scope of this research is to study flow patterns and temperature profile inside the air duct and to simplify the temperature profile for optimization of the system performance

1.5 Relevancy and Feasibility of Study

The limited number of thermocouple and other measuring device attached to the system makes it difficult to observe what is happening inside the duct. As a solution of the problem, using as much as many constraint in geometry modelling available in the simulation software and taking into considerations all parameter obtained from the experimental setup to resemble the system and predict flow pattern inside the air duct.

This simulation requires steps to adhere to and proper parameter to be set in order for the simulation to solve for a converged solution. The project can be completed in time, given every error can be solve and the value from the experiment is applicable in the simulation.

CHAPTER 2

LITERATURE REVIEW

2.1 ThermoElectric Cooler System

In 1821, thermo-electrics effect cause by thermal gradient formed between two dissimilar conductors was discovered by Thomas Johann Seebeck [2]. This temperature differences conversion into electricity is the call Seebeck effect. Semiconductor material inside a Peltier effect device are solid-state energy converters that can generate heat (or removed) at the junction when electrical current applied to the material [3].

A TEMs is a circuit containing thermoelectric materials arranged in certain configurations that either generate electricity from direct heat or convert electricity into temperature gradient [4]. As illustrated in Figure 2.1, TECs (thermoelectric coolers) using TEMs to transfer the heat rejected which normally installed with a heat sink to dissipate the heat to the environment. Cold plate side where the heat is absorbed cause the enclosure temperature at the side to reduce. For higher temperature gradient required, the modules can be arranged into multiple columns and rows to achieve the effect.

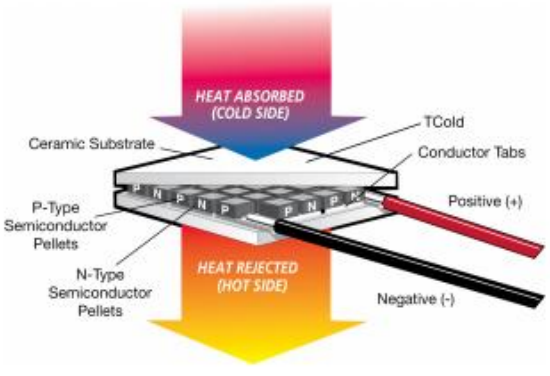

Figure 2.1 A Thermoelectric Module [5].

In the early 1900's, metals were still considered to exhibit the best thermoelectric properties. It had been shown mathematically that a good thermoelectric material should have a high Seebeck coefficient, high electrical conductivity, and low thermal conductivity. These characteristics minimize the thermal effects of Joule heating and dampen the effects of the parasitic heat path which is opposite the direction of heat pumping. In quantitative terms, it was shown that practical refrigeration and power generation would be possible with materials, which hadn't been invented yet, possessing optimal properties.

With the invention of the transistor, in 1949, came a new type of material called the semiconductor. It was found that semiconductors could meet the parametric needs far better than metals, and a new material, bismuth telluride (Bi2Te3) was developed and found to have advantageous properties near room temperature. Also, because we typically operate a thermoelectric device thermally in parallel, and electronically in series, there is a necessity to have materials that transport heat in opposite directions with respect to current direction. Bi_2Te_3 is given the ability to be used for the two inversely related branches by doping it into extrinsic semiconductors.

Due to the state of materials sciences at the time, thermoelectric refrigeration and power generation efficiencies were significantly worse than their vapor-compression counterparts. Thermocouples, on the other hand, do not require efficient thermal to electric energy transformation. For this reason, they have been used and developed for much longer than Thermoelectric generator and cooler. As materials sciences advanced, increased efficiencies translated to using ThermoElectric Devices (TED's) in commercial and industrial applications requiring small dimensions, gravity independence, and a solid state/maintenance free design.

In the analysis of TEMs, four different heat effects can be described. These are Peltier cooling, Peltier heating, Joule heat, and Fourier heat. Joule heat, occurs when the electrical current is passed through an electrical resistance. It is accepted that half of this heat is transported from the cold surface and the other part is transported from the hot surface. Fourier heat, can be defined as the heat transfer from hot surface to cold surface by conduction.

To achieve a satisfactory thermal comfort there are many limitations to which TEC is able to operate efficiently. TEC performance are measured with the flexibility

of the system to balance the heat transfer by the modules and the ability to optimize the temperature difference between the enclosure area and the ambient temperature. The main problem in TEC is to reduce the heat flux across the hot and the cold space that mostly occurs in the material which separates the flow in the air duct system.

High capital cost and poor power performance of TEC causing current applications of thermoelectric technology restricted for large enclosure cooling [6]. Other restrictions includes:

- Fluctuating environment.
- Small scale cooling
- Small temperature gradient
- Reversible heating and cooling using same modules
- Space constraints

Thermoelectric cooling will be considered economically feasible if the coefficient of performance is about average of vapour compression cooling or higher [7]. Compared to vapour compression cooling which uses rotating equipment in the compressor, TEC have no moving parts thus results to higher reliability and noise free operation. TEC cooling can operate using compact and smaller equipment with higher cooling density. Reversible heating and cooling can be achieved using same modules by reversing the electrical current flow. Besides, the cooling power can be control proportional to input power. TEC is flexible in design to meet particular requirements and refrigerant free system.

2.2 ThermoElectric Configurations

The temperature of the cold side and the cooling capacity of a TEC can be decreased by multistage TECs. An analytical method was developed for two-stage TECs for predicting the performance of the module [8]. The performance of a refrigerator with multistage TECs was investigated by Pan et al. [9]. The performance comparison of single-stage and multistage TECs was investigated [10]. A three-dimensional model was developed for the performance optimization of two-stage TECs [11]. Putra et al. [12] investigated the performance of 5- and 6- stage TECs for cryogenic applications.

2.3 ThermoElectric Applications

One of earliest application of TECs are made for cooling small enclosure [13]. In France, thermoelectric cooling for thermal comfort are used in railroad cabs and submarines. Under operating condition of 3 ampere, experimental findings of a lab-scale ceiling, natural convection type TE-AC (thermoelectric air conditioning) with a natural convection on fin at the cold side and a forced heat convection at the heat sink at the hot side of the TEMs, the experiment accomplished maximum cooling capacity of 169 W.

An investigation of thermoelectric air-conditioners compared to vapour compression and absorption air-conditioner made shows that TE-AC have the highest purchasing and operating cost under same period of time with highest efficiency at COP of 0.38-0.45 [14]. A compact TE-AC experiment conducted under operating condition of 1 A, the cooling capacity of 29 W is achieved. The experiment setup meets the requirement of 80% acceptability criteria with ANSI/ASHRAE Standard 55 (standard for indoor thermal comfort) with coefficient of performance of 0.34 [15].

Cosnier et al. [16] experimentally studied model of a TEC system using a series of TEMs. The cold side of the modules is attached with fins forced convected to the air circulation while the hot sides are in contact with heat sink with fluid as the medium. Operating under 4 ampere the coefficient of performance of 1.5 to 2 is achieved, with cooling capacity of 50 W per module. Khire et al [17] proposed TEC to be implemented for cooling of building envelope for domestic level.

These studies highlight the benefit of the PVMs (photovoltaic modules) to supply the power to TEC [18]. Kraemer et al. [19] stated that solar cells does not optimize the lower solar radiation frequency. Several design have been patented using abundant heat energy from solar radiation to its advantage in thermoelectric applications. Wahab et al. [20] designed and tested a solar thermoelectric refrigerator. According to the results, the inside temperature of the refrigerator was decreased from 27°C to 5°C in 44 minutes with a COP of 0.16. Dai [21] also found that the COP value of a photovoltaic driven TEC was approximately 0.3. Min and Rowe [4] showed that, for 5°C refrigerator inside temperature and 25°C environment temperature, the COP value of the thermoelectric refrigerator was between 0.3 and 0.5. Khattab and El Shenawy [22] investigated to drive TECs by TEGs. It was shown that five TEGs were able to drive one TEC for Egypt climatic conditions.

Yilmazoglu [23] numerical model for prototype thermoelectric heating and cooling unit is investigated under various TEC voltage differences. Temperature gradient of 9.1°c and 2.8°c occurred in the hot and cold side air duct.

Different studies made to this day shown that for small scale air-conditioning system using TEMs technology make it feasible to do small cooling job. A number of studies suggest application TEMs for small-scale air condition to be powered by PVMs.

2.4 CFD Simulation Validation and Verification.

Verification and validation provide a framework for rigorously assessing the accuracy of CFD simulations. Verification deals purely with the mathematics of a chosen set of equations and can be thought of as solving the equations right. Validation, on the other hand, entails a comparison to experimental data, that is, real-world observations, and is concerned with solving the right equations. With regards to the sequence, verification must be performed first for quantitative validation comparisons to be meaningful. Error types that are quantified in verification activities include coding errors, that is, mistakes, incomplete iterative convergence error, round off error, far-field boundary error, temporal convergence error, and grid convergence (or discretization) error. This last source of error is related to the adequacy of the computational mesh employed and is the focus of the current effort.

Carpenter et al. conducted a careful study of the grid convergence behaviour for a two-dimensional hypersonic blunt-body flow [24]. Their study employed higher-order methods and omitted any flux limiting at the shock wave. Although the numerical schemes they employed were formally third and fourth order, they found that the spatial order of accuracy always reverted to first order on sufficiently refines meshes. Their findings indicate that even without the use of flux limiters to reduce the spatial order of accuracy at discontinuities, the information is passed through the shock wave in a first-order manner (at least in two dimensions and higher). Similar results have been observed by other authors.

Previous work by Roy et al. and Roy verified the presence of both first- and second-order errors for a laminar hypersonic blunt body flow when a formally second-order numerical scheme was used in conjunction with flux limiting at the shock wave.

It was shown that the use of a mixed-order numerical scheme resulted in non-monotonic convergence of certain flow properties as the mesh was refined. This nonmonotonic grid convergence behaviour was found to occur when the first- and second-order error terms were of opposite sign, thus leading to error cancellation. Nonmonotonic grid convergence has been observed by a number of other authors. For example, Celik and Karatekin examined the flow over a backward-facing step using the k–ε turbulence model with wall functions [25]. These authors found significant nonmonotonicity in both the velocity and turbulent kinetic energy profiles as the grid was refined. The main goal of this work is to explore, in detail, the behaviour of a mixed first- and second-order numerical scheme as the grid is refined. A secondary goal is to develop an error estimator that can be applied to such schemes. The test problem used is the Mach 8 inviscid flow of a calorically perfect gas (° D 1.4) over a spherically blunted cone. This flow field contains a strong bow shockwave where the formally second-order spatial discretization reduces to first order.

CHAPTER 3

METHODOLOGY

The methodology describes the flow of this study process in achieving optimized solution for the TE-AD system.

3.1 Research Methodology Procedure

Shown in Figure 3.1, is the summary of the process involved in this study.

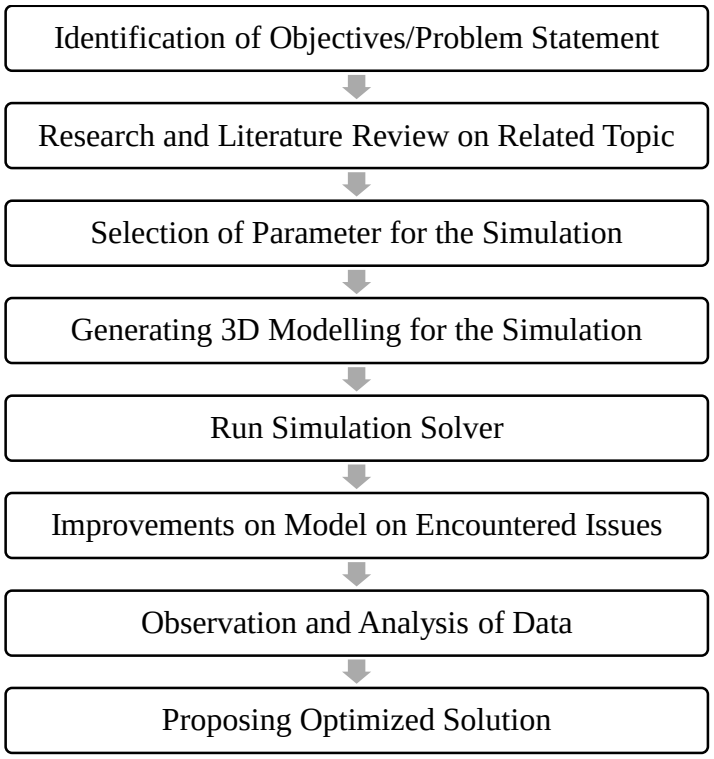

Figure 3.1 Research Methodology Flow Process.

Project Activities

Figure 3.2 explains the summary of the project activities required in completing this study while Figure 3.3 describes the computation flow inside the simulation software.

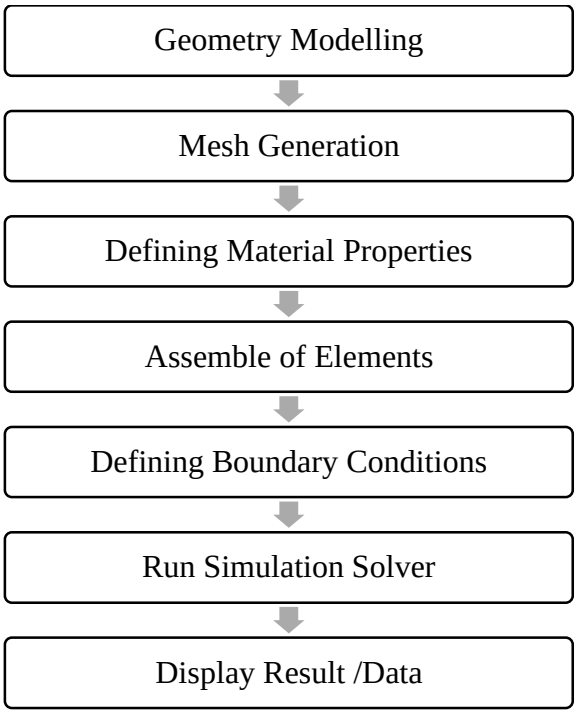

Figure 3.2. Project Activities

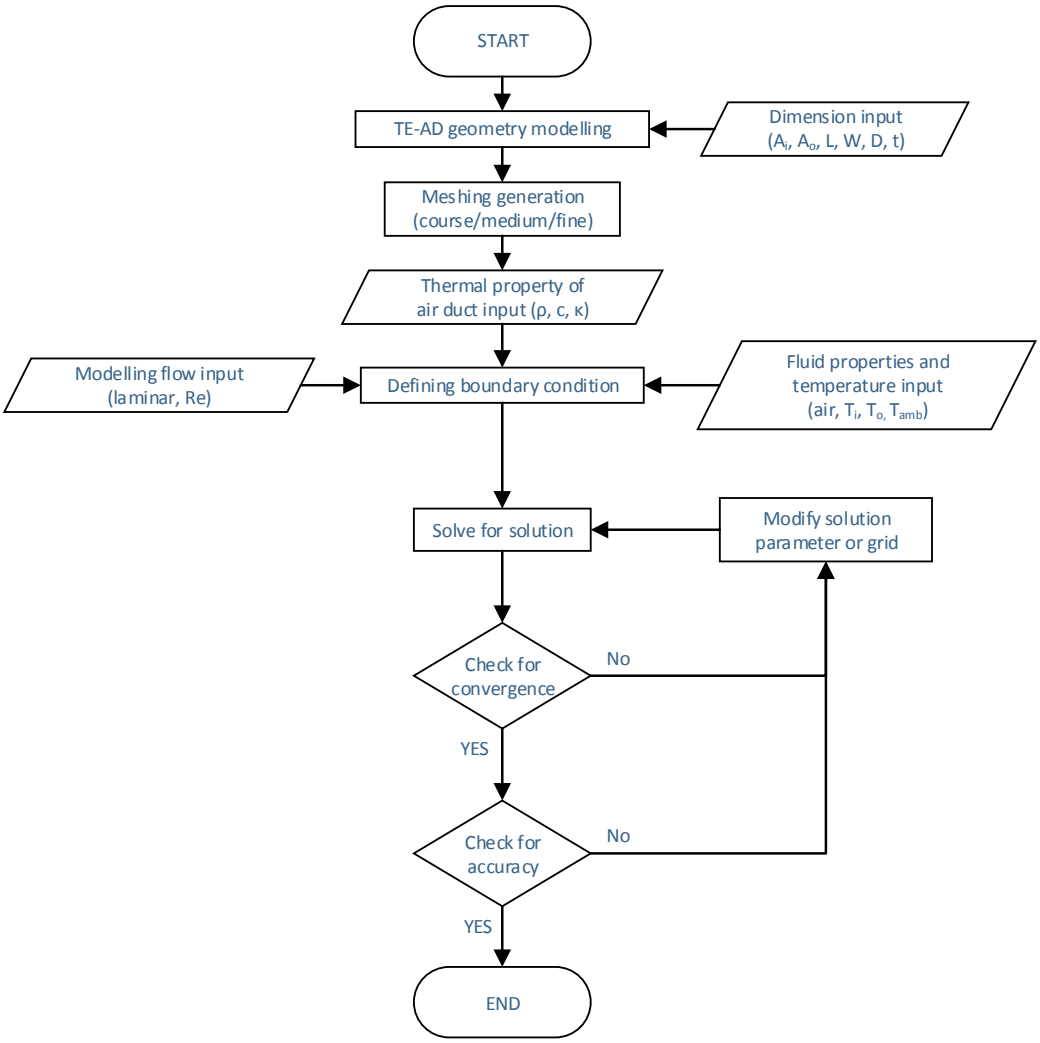

Figure 3.3. Simulation Work Flow Chart (ANSYS Fluent)

3.2 Tools and Equipment

ANSYS computational fluid dynamics (CFD) Fluent simulation software and Microsoft Excel is utilized to predict the impact of fluid flow throughout the TE-AD system.

3.3 Project Key Milestones

- Phase I

  - CFD Simulation (Week 11-19)

- Phase II

  - Mesh Independence Study (Week 14-20)

3.4 Project Gantt Chart

Table 3.1. Project Gantt Chart

Activity	Week																											
	FYP 1														FYP 2													
	1	2	3	4	5	6	7	8	9	10	11	12	13	14	15	16	17	18	19	20	21	22	23	24	25	26	27	28
Project Title Selection																												
Preliminary Research																												
Research on TE-AD																												
Analysis on common boundary condition																												
Software familiarization																												
CFD Simulation																												
Mesh Independence Study																												
Data Analysis																												
Problem Resolution																												
Result evaluation and discussion																												

3.5 Experimental Setup

It was noted that at an applied voltage of 5 V and input current of 6 A, each TEM module generates 25 W cooling power. Thus, for a cooling load of 589 W, the number of TEMs required was 24 units which can provide up to 600 W of cooling power at the given configuration, which was slightly higher than the required cooling load. The ambient air was circulated inside the test room via the TE-AD system installed on the north side of the room with the help of a fan as shown in Figure 3.5.

3.5.1 Test Room

Stated by Irshad et. al the experimental process and data collection was conducted at 4°23'11"N 100°58'47"E, Perak, Malaysia under tropical climate. The test room dimension is 2.8 m wide, 2.7m deep, and 2.5m high as shown in Figure 3.4. The test room installed with windows (0.304m x 0.22m) with a door (0.821m x 2m).

Figure 3.4. Test room equipped with TE-AD [26]

3.6 Thermoelectric Air Duct Description

The TE-AD is mounted on the wall of the building envelope exterior. The modules arranged in 8 rows and 3 columns in Figure 3.5. The entire face of the air duct are built using aluminium sheet with a frame as the foundation. Aluminium foil is wrapped around the air duct to act as the insulation to reduce the heat flux between the duct enclosure and the ambient space.

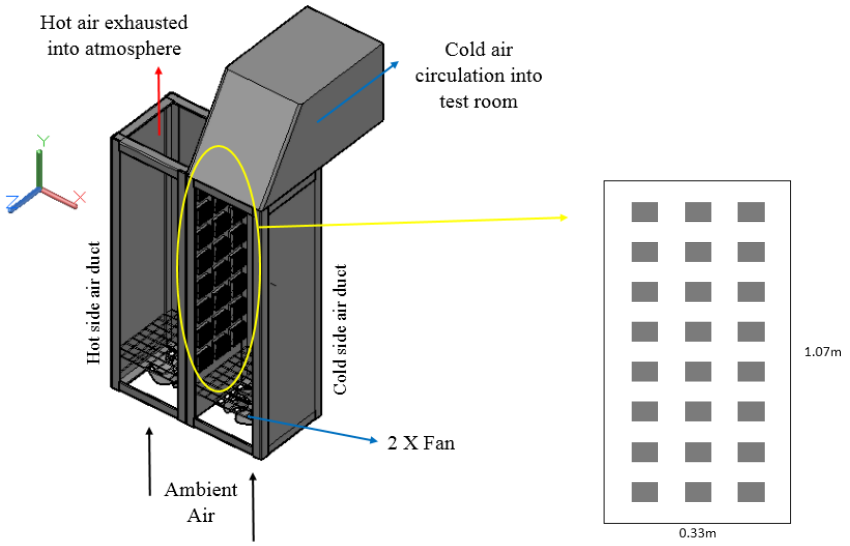

Figure 3.5. Breakout Section View of TE-AD

Table 3.2. Range of geometrical and operating parameters for CFD analysis.

Geometrical parameters	Range
Entrance length of duct /mm	1070
Width of duct /mm	330
Depth of duct /mm	330
Duct aspect ratio (W/H)	1

3.7 Governing Equation.

The numerical model for fluid flow and heat transfer through an air duct is developed under the following assumptions:

1. The fluids maintain single-phase, incompressible turbulent flow across the duct.
2. Steady 2D fluid flow and heat transfer.
3. Both thermally and hydraulically fully developed flow (steady-state conditions).
4. The thermo-physical properties of both the fluid (air) and the cold plate (aluminum) are constant (temperature independent).
5. Negligible radiation heat transfer

The CFD methods consist of numerical solutions of mass, momentum and energy conservation with other equations like species transport. The solution of these equations accomplishes with numerical algorithm and methods. The governing equations are summarized as follows:

Continuity equation

$$\frac{\partial}{\partial x_i}(\rho u_i) = 0 \qquad [3.1]$$

Momentum equation

$$\frac{\partial}{\partial x_i}(\rho u_i u_j) = -\frac{\partial p}{\partial x_i} + \frac{\partial}{\partial x_j}\left[\mu\left(\frac{\partial u_i}{\partial x_j} + \frac{\partial u_j}{\partial x_i}\right)\right] + \frac{\partial}{\partial x_j}\left(-\overline{\rho \acute{u}_i \acute{u}_j}\right) \qquad [3.2]$$

Energy equation

$$\frac{\partial}{\partial x_i}(\rho u_i T) = \frac{\partial}{\partial x_j}\left[(\Gamma + \Gamma_t)\frac{\partial T}{\partial x_j}\right] \qquad [3.3]$$

Where Γ and Γt are molecular thermal diffusivity and turbulent thermal diffusivity, respectively and are given by

$$\Gamma = \frac{\mu}{P_r} \; and \; \Gamma_t = \frac{\mu_t}{Pr_t} \qquad [3.4]$$

Energy transport equation:

$$\frac{\partial(\rho E)}{\partial t} + \nabla.\left[\vec{V}(\rho E + \rho)\right] = \nabla.\left[k_{eff}\nabla T - \sum_j h_j J_j + \left(\overline{\overline{\tau_{eff}}}.\vec{V}\right)\right] + S_h \qquad [3.5]$$

Energy E per unit mass is defined as:

$$E = h - \frac{p}{\rho} + \frac{V^2}{2} \qquad [3.6]$$

Pressure work and kinetic energy are always omitted for with compressible flows when using the pressure-based solvers.

Setting the simulation as conjugate heat transfer setup, the software is able to compute conduction of heat through solids, coupled with convective heat transfer in fluid. And the Coupled boundary condition is assigned to the air duct wall zone which separates two cell zones, the solid (aluminium sheet housing and cold plate) and fluid (mixed air template).

3.7.1 Standard k-ε Model

Turbulence energy k has its own transport equation:

$$\frac{\partial(\rho k)}{\partial t}+\frac{\partial(\rho \bar{u}_i k)}{\partial x_i}=-\overline{\rho \acute{u}_i \acute{u}_j}\frac{\partial \bar{u}_i}{\partial x_j}-\rho\varepsilon+\frac{\partial}{\partial x_j}\left[\left(\mu+\frac{\mu_t}{\sigma_k}\right)\frac{\partial k}{\partial x_j}\right] \quad [3.7]$$

This requires a dissipation rate, ε, which is entirely modeled phenomenologically (not derived) as follows:

$$\frac{\partial(\rho\varepsilon)}{\partial t}+\frac{\partial(\rho \bar{u}_i \varepsilon)}{\partial x_i}=\frac{\partial}{\partial x_j}\left[\left(\mu+\frac{\mu_t}{\sigma_\varepsilon}\right)\frac{\partial \varepsilon}{\partial x_j}\right]+\mathrm{C}_{1\varepsilon}P_k\frac{\varepsilon}{k}-\mathrm{C}_{2\varepsilon}\rho\frac{\varepsilon^2}{k} \quad [3.8]$$

Dimensionally, the dissipation rate is related to k and a turbulence length scale:

$$\varepsilon\sim\frac{k^{3/2}}{L_t} \quad [3.9]$$

Together with the k equation, eddy viscosity can be expressed as:

$$\mu_t=\rho\mathrm{C}_\mu L_t\sqrt{k}=\rho\mathrm{C}_\mu\frac{k^2}{\varepsilon} \quad [3.10]$$

3.8 Simulation Work

For simulation work is simplified the air duct into geometry of a rectangle (0.33m x 1.07m) in Figure 3.6 and were done separately for cold air stream and hot air stream inside the air duct. Aluminium housing is model as a Thin Wall model (Figure 3.6). In this case, meshing the lower solid zone for the wall is not required. Thin wall model applies normal conduction only (no in-plane conduction) and no actual cells are created. Wall thermal boundary condition is applied at the outer layer.

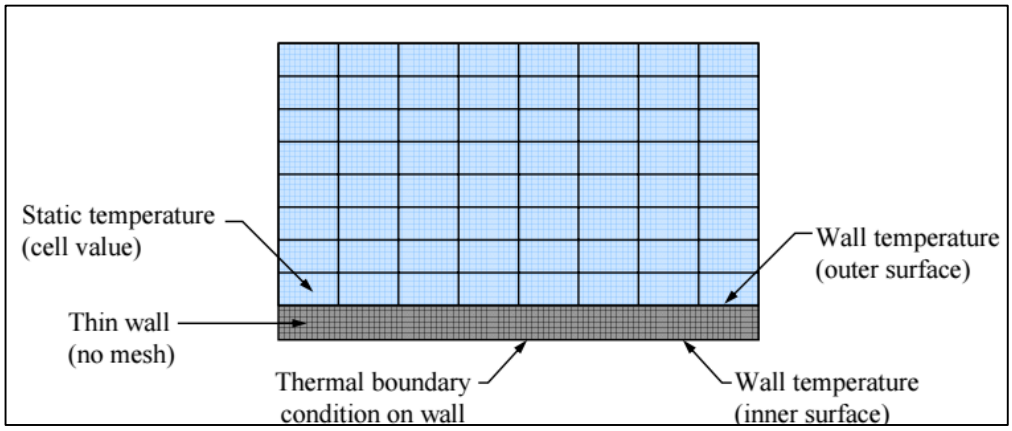

Figure 3.6. Temperature Definitions for Thin Wall Model

Natural convection occurs when heat is added to fluid and fluid density varies with temperature. Flow is induced by force of gravity acting on density variation. When gravity term is included, pressure gradient and body force term in the momentum equation are re-written as:

$$-\frac{\partial p}{\partial x} + \rho g \rightarrow \frac{\partial \acute{p}}{\partial x} + (\rho - \rho_0)g \quad [3.11]$$

Where,

$$\acute{p} = p - \rho_0 g x \quad [3.12]$$

The meshing generation is created by using coarse relevant centre on the geometry used to "fill" the solid model with nodes and elements creating minimum and maximum size of 0.5mm and 100mm relatively. The meshing is concentrated on the TEMs side of the air duct. By using these explicit sizing controls, the resolution of the geometry can be accurately captured and to ensure that it is accurately resolve any high gradient areas in the flow, such as a wake or separation/recirculation zones. Solutions compute by the simulation are done at nodes (Nodal solutions). The higher the number of elements (mesh density), the better the solution approaches the exact solution. Although the solution time increases with the increase of elements, the mesh is balanced with time available and accuracy needed. The faces of the geometry are named as shown in Figure 3.7.

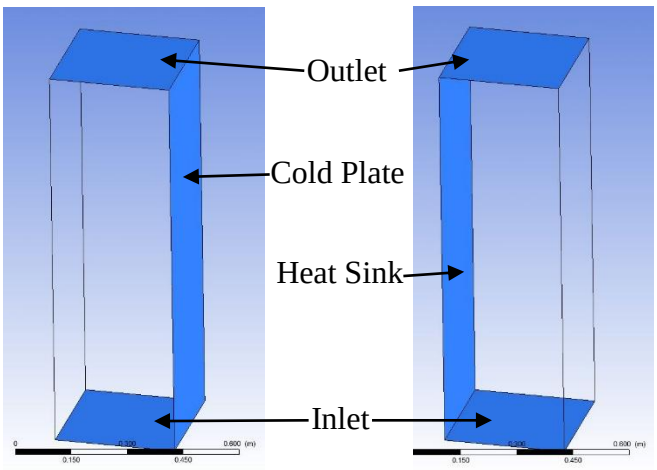

Figure 3.7. Named Selections

Using species transport model with energy equation and standard k-ε turbulence model, the boundary conditions set up are as below Table 3.3. Boundary Conditions

Table 3.3. Boundary Conditions

Operating Parameter	Range
Cold plate temperature	283.15 k
Heat sink temperature	400k
Inlet velocity Magnitude	0.5 m/s
Outlet gauge pressure	1 atm
Insulated wall heat flux	0 w/ m^2
Insulation Sheet External emissivity	0.03

Before the simulation is started, grid check is performed to avoid problems due to incorrect mesh connectivity and maximum cell skewness are observed to be below 1. All physical dimensions are initially assumed to be in meters. The model grid are scaled accordingly. Energy underrelaxation factor are set between 0.95 and 1, because for problems with conjugate heat transfer, when the conductivity ratio is very high, smaller values of the energy underrelaxation factor practically stall the convergence rate. For problems with conjugate heat transfer, when the conductivity ratio is very high, smaller values of the energy underrelaxation factor practically stall the convergence rate.

Node-based gradients with unstructured tetrahedral meshes is used. The node-based averaging scheme is known to be more accurate than the default cell-based scheme for unstructured meshes, most notably for triangular and tetrahedral meshes [1]. While monitoring convergence with residuals history, residual plots can show when the residual values have reached the specified tolerance. After the simulation, residuals have decreased by at least 3 orders of magnitude to at least 10^{-3}. For the segregated solver, the scaled energy residual must decrease to 10^{-6}. Also, the scaled species residual may need to decrease to 10^{-5} to achieve species balance.

To conclude, the simulation was solved under steady state conditions with pressure-based solver and operating conditions of negative gravitational acceleration in y-axis direction. Energy equation, standard k-ε turbulence and species transport model were used. Both simulation, the solution converged under 300 number of iterations performed by SIMPLE algorithm.

Chapter 4

Result and Discussions

4.1 Mesh Independence Study

Grid convergence is the term used to describe the improvement of results by using successively smaller cell sizes for the calculations. A calculation should approach the correct answer as the mesh becomes finer, hence the term grid convergence. The normal CFD technique is to start with a coarse mesh and gradually refine it until the changes observed in the results are smaller than a pre-defined acceptable error.

The initial simulation is solved using initial mesh and keep refining the mesh until convergence criteria was reached. The second simulation is solved by refining the mesh globally. A set of temperature data is recorded at four point across the air duct shown in Figure 4.1.

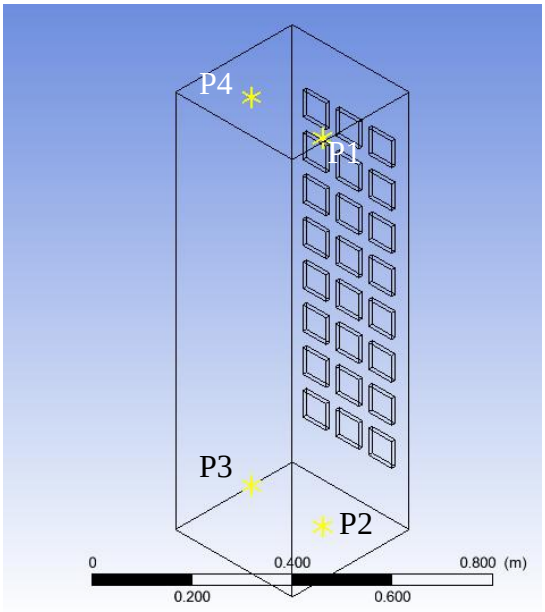

Figure 4.1. Temperature Data Point

Illustrated in Figure 4.2, by increasing the mesh size further, 0.4-0.5 million elements simulation results in a value that is within a constant range. Solution value that is independent of the mesh resolution is reached. Only the result obtained from

the simulation meshing generation with no of elements above 400k is acceptable. This step is applied for every simulation computed in the ANSYS Fluent.

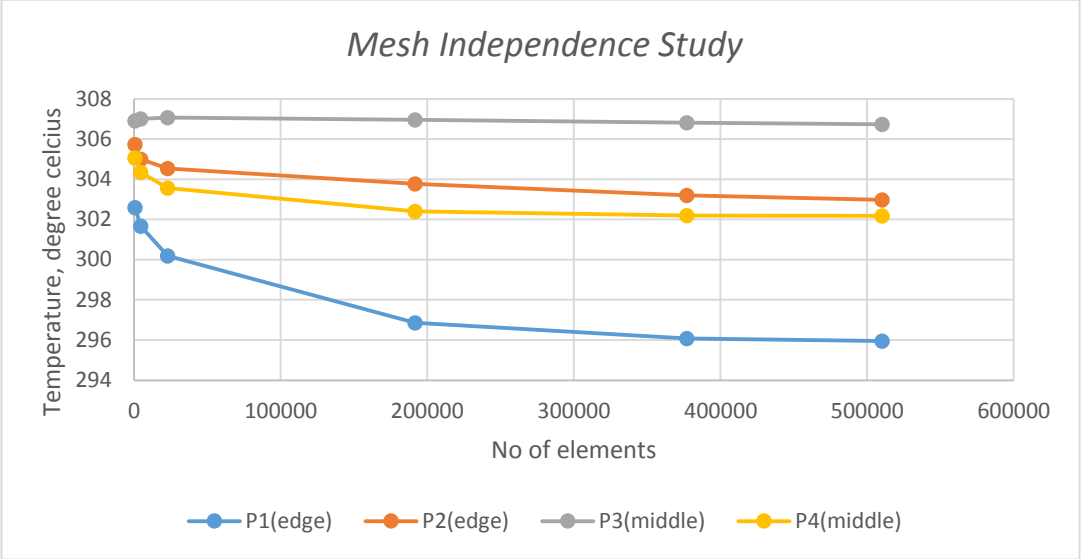

Figure 4.2. Mesh Independence Study.

4.2 Effects of the TE-AD system on temperature gradient.

The summary of the temperature profile calculation are as shown in Table 4.1. Temperature Contour Calculation. Refer to Appendix 5 for the temperature contour inside the air duct.

Table 4.1. Temperature Contour Calculation

Air Duct	Cold	Hot
Temperature (min), K	283.2	307.2
Temperature (max), K	307.2	400
Average Temperature (Inlet), K	307.2	307.2
Average Temperature (Outlet), K	303.4	310.1
Temperature gradient between Inlet and Outlet, K	3.8	2.9

4.3 Effects of the TE-AD system on pressure and air velocity.

The specified boundary conditions for air velocity and outlet pressure cause the solutions to solve the simulation under constant pressure and velocity in Figure 4.3.

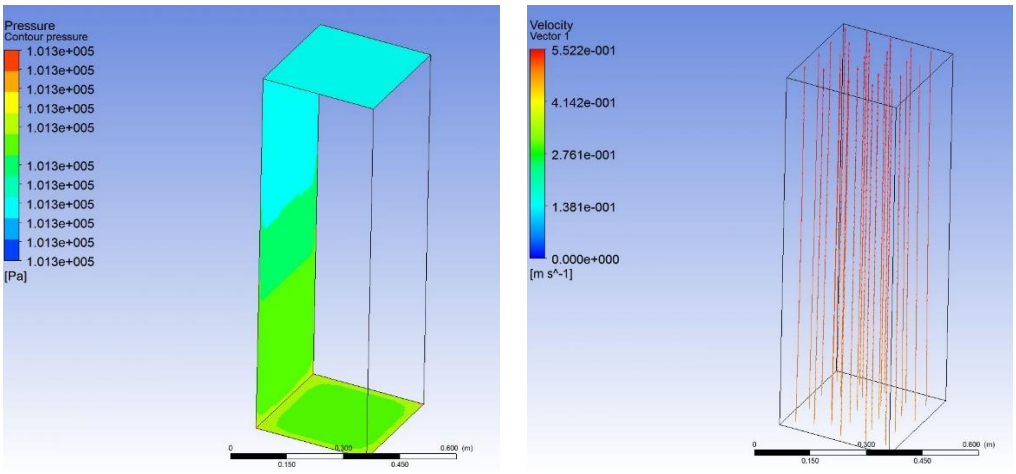

Figure 4.3. Pressure and Air Velocity Contour for Hot and Cold air duct

4.4 Effects of different air velocity on temperature gradient.

Using plane distributed along the air duct, the average temperature on each plane is taken in Figure 4.4.

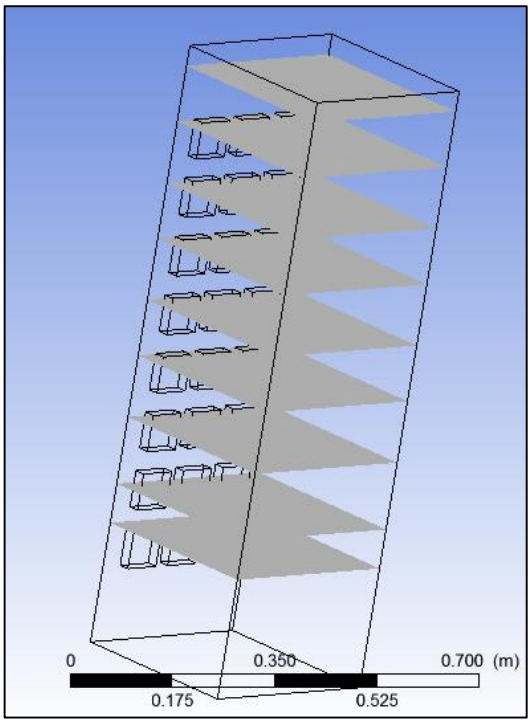

Figure 4.4. Data Plane in the air duct.

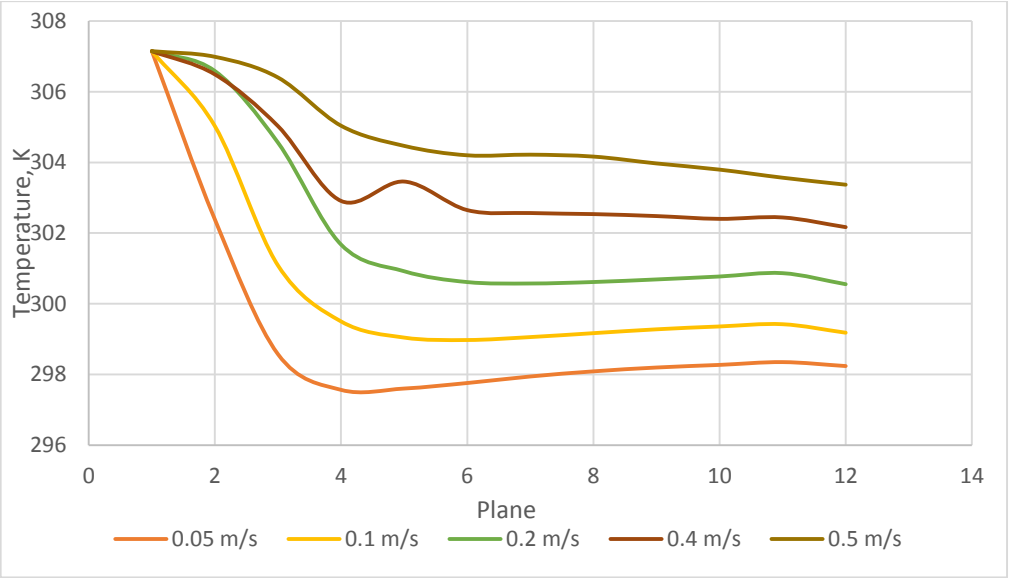

Figure 4.5. Temperature distribution across data plane for various inlet velocity.

The effect of air velocity on temperature gradient measured in cold air duct was investigated. In Table 4.2, for different air velocity the temperature gradient vary between 8.913 and 2.297 degrees.

Table 4.2. Temperature Gradient for Different Air Velocity

Inlet Velocity,m/s	0.05	0.1	0.2	0.3	0.4	0.5
Temperature Gradient, degree	8.913	7.969	6.596	4.981	3.78	2.297

4.5 Comparison of simulation and experimental results.

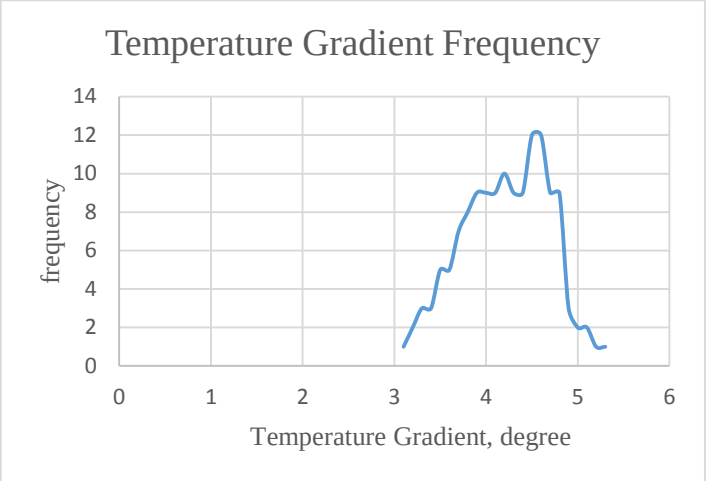

Figure 4.6. Variation of temperature gradient when the TE-AD system operated at 5-6 A from experimental study [26].

To calculate the mean of distribution,

$$\mu = \sum [x.P(x)] \qquad [4.1]$$

The simulated and the experimental results of the TE-AD system were compared and found in good agreement. Since the optimum performance of the TE-AD system was found in the current range of 5-6 A under inlet velocity of 0.4 m/s, so experimental results of indoor temperature for this range were compared with simulated results and presented in Table 4.3. Results show that the temperature difference between experimental and simulation data was less than ±0.4 °C.

Table 4.3. Comparison of experimental and simulation data

	Experimental	Simulation
Temp. gradient, °C	4.2	3.8
Percentage error, %	9.5	

CHAPTER 4

CONCLUSION AND RECOMMENDATION

The purpose of the simulations is to replicate the same setup as the experimental and to observe the behaviour of the performance under different conditions. The TE-AD simulation model provide detailed temperature profiles in the air duct and velocity contours as well as the temperature drop in the air duct. In comparison to the benchmark experimental analyses, the results validate the accuracy of the simulation model. According to the simulation study, it was possible to cool down air flows by 4°C for the assigned boundary conditions. The study shows that it is possible to use TECs as an alternative method for HVAC applications with properly designed air duct system.

Nonetheless, the verification and validation procedures and methodology are recommended for use. Use of such procedures and methodology should be helpful in guiding future developments in CFD through documentation, verification, and validation studies and in transition of CFD codes to design through establishment of credibility. Presumably, with a sufficient number of documented, verified, and validated solutions along with selected verification studies a CFD code can be accredited for a certain range of applications. The contribution of the present work is in providing procedures and methodology for the former, which hopefully will help lead to the better future simulation. Although validation is made for assessing the model uncertainty by using the experimental data under same operating conditions, much more work can be integrated into the simulation for additional error source and alternative error by using user defined function for the temperature input and material selection to account for fluctuating environment and different materials of the air duct for the system optimization.

As suggested by many previous study, integrating this TE-AD system with photovoltaic modules provide utilization of solar energy, especially in cooling applications in tropical climate.

References

[1] "ANSYS Release 9.0 Documentation," 2004. [Online].

[2] W. R. Fahrner and S. Schwertheim, "Semiconductor thermoelectric generators," Stafa-Zuerich, Trans Tech, 2009.

[3] G. S. Nolas and J. Sharp, "Historical Development," *Thermoelectrics: basic principles and new materials developments*, pp. 1-33, 2001.

[4] D. M. Rowe, "Thermoelectric Module Design Theories," in *Thermoelectrics handbook macro to nano*, Boca Raton, CRC/Taylor & Francis, 2006, pp. 1-16.

[5] "Frequently Asked Questions About Our Cooling And Heating Technology," [Online]. Available: http://tellurex.com/wp-content/uploads/2014/04/peltier-faq.pdf. [Accessed October 2015].

[6] D. R. Brown, J. A. Dirks, N. Fernandez and T. E. Stout, "The Prospects of Alternatives to Vapor Compression Technology for Space Cooling and Food Refrigeration Applications," 2010.

[7] L. G. Stokholm, "Reliability of thermoelectric cooling systems," in *Proceedings of Xth International Conference on Thermoelectrics*, Cardiff, 1991.

[8] M. Ma and J. Yu, "An analysis on a two-stage cascade thermoelectric cooler for electronics cooling applications," *International Journal of Refrigeration*, no. http://dx.doi.org/10.1016/j.ijrefrig, 2013.

[9] Y. Pan, B. Lin and J. Chen , "Performance analysis and parametric optimal design of an irreversible multi-couple thermoelectric refrigerator under various operating conditions," vol. 84, pp. 882-892, 2007.

[10] G. Karimi, J. Culham and V. Kazerouni, "Performance analysis of multi-stage thermoelectric coolers," *International Journal of Refrigeration*, vol. 34, pp. 2129-2135, 2011.

[11] X. Wang, Q. Wang and J. Xu, "Performance analysis of two-stage TECs (thermoelectric coolers) using a three dimensional heat-electricity coupled model," *Energy*, no. energy.2013.10.047, 2013.

[12] N. Putra, A. Sukyono, D. Johansen and F. Iskandar, "The characterization of a cascade thermoelectric cooler in a cryosurgery device, Cryogenics," vol. 50, pp. 759-764, 2010.

[13] J. Stockolm, L. Pujol-Soulet and P. Sternat, "Prototype thermoelectric air conditioning of a passenger railway coach," in *4th Intern Conf on Thermoelectric Energy Conversion*, Arlington, 1982.

[14] S. Riffat and G. Qiu, "Comparative investigation of thermoelectric air-conditioners versus vapour compression and absorption air-conditioners," *Applied Thermal Engineering*, vol. 24, p. 1979–1993, 2004.

[15] S. Maneewan, W. Tipsaenprom and C. Lertsatitthanakorn, "Thermal Comfort Study of a Compact Thermoelectric Air Conditioner," *Journal of Electronic Materials*, vol. 39, p. 1659–1664, 2010.

[16] M. Cosnier, G. Fraisse and L. L, "An experimental and numerical study of a thermoelectric air-cooling and air-heating system," *International Journal of Refrigeration*, vol. 31, pp. 1051-1062, 2008.

[17] R. Khire, A. Messac and S. VanDessel, "Design of thermoelectric heat pump unit for active building envelope," *International Journal of Heat and Mass Transfer*, vol. 48, p. 4028–4040, 2005.

[18] S. Van, "Feasibility of photovoltaic-Thermoelectric hybrid modules," *Applied Energy*, vol. 88, pp. 2785-2790, 2011.

[19] D. Kraemer, L. Hu, A. Muto, X. Chen, G. Chen and M. Chiesa, "Photovoltaic-thermoelectric hybrid systems:A general optimization methodology," *Appl. Phys. Lett. Applied Physics Letters*, p. 243503, 2008.

[20] S. Abdul Wahab, A. Elkamel , A. Al-Damkhi, I. Al-Habsi, H. Al-Rbai'ey, A. Al-Battashi, A. Al-Tamimi, K. Al-Mamari and M. Chutani, "Design and

experimental investigation of portable solar thermoelectric refrigerator," *Renewable Energy,* vol. 34, pp. 30-34, 2009.

[21] Y. Dai, R. Wang and L. Ni, "Experimental investigation and analysis on a thermoelectric refrigerator driven by solar cells," *Solar Energy Materials & Solar Cells,* vol. 77, pp. 377-391, 2003.

[22] N. Khattab and E. El Shenawi, "Optimal operation of thermoelectric cooler driven by solar thermoelectric generator," *Energy Conversion and Management,* vol. 47, pp. 407-426, 2006.

[23] M. Yilmazoglu, "Experimental and numerical investigation of a prototype thermoelectric heating and cooling unit," *Energy and Buildings (2015),* no. http://dx.doi.org/10.1016/j.enbuild.2015.12.046.

[24] M. Capenter and J. Casper, "Accuracy of Shock Capturing in Two Spatial Dimensions," *AIAA Journal,* vol. 37, no. 9, pp. 1072-1079, 1999.

[25] I. Celik and O. Karatekin, "Numerical Experiments on Application of Richardson Extrapolation with Nonuniform Grids," *Journal of Fluids Engineering,* vol. 119, no. 3, pp. 584-590, 1997.

[26] K. Irshad, K. Habib, N. Thirumalaiswamy and B. B. Saha, "Performance analysis of a thermoelectric air duct system for energy-efficient buildings," *Energy,* pp. 1009-1017, 2015.

[27] M. A. Ghazali and R. A. M. Abdul, "The Performance of Three Different Solar Panels for Solar Electricity Applying Solar Tracking Device under the Malaysian Climate Condition," *Energy and Environment Research,* 2012.

APPENDICES

Appendix 1: Simulation Meshing Generation

Model (B3) > Mesh

Object Name	*Mesh*
State	Solved
Defaults	
Physics Preference	CFD
Solver Preference	Fluent
Relevance	0
Sizing	
Use Advanced Size Function	On: Curvature
Relevance Center	Coarse
Initial Size Seed	Active Assembly
Smoothing	High
Transition	Slow
Span Angle Center	Coarse
Curvature Normal Angle	Default (70.3950 °)
Min Size	0.50 mm
Max Face Size	50.0 mm
Max Size	100.0 mm
Growth Rate	1.20
Minimum Edge Length	10.0 mm

Advanced	
Number of CPUs for Parallel Part Meshing	Program Controlled
Shape Checking	CFD
Element Midside Nodes	Dropped
Straight Sided Elements	
Number of Retries	0
Extra Retries For Assembly	Yes
Rigid Body Behavior	Dimensionally Reduced
Mesh Morphing	Disabled
Defeaturing	
Pinch Tolerance	Default (0.450 mm)
Generate Pinch on Refresh	No
Automatic Mesh Based Defeaturing	On
Defeaturing Tolerance	Default (0.250 mm)
Statistics	
Nodes	99360
Elements	494955
Mesh Metric	Aspect Ratio
Min	1
Max	9.9946
Average	1.83220063116847
Standard Deviation	0.47603011035999

Appendix 2: Simulation Mesh

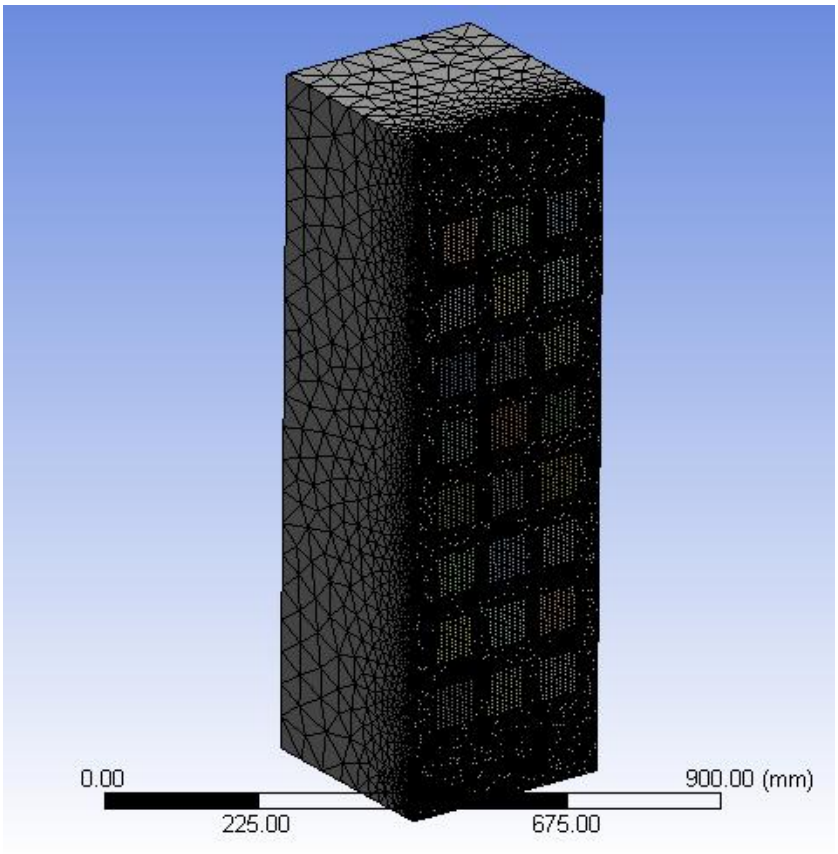

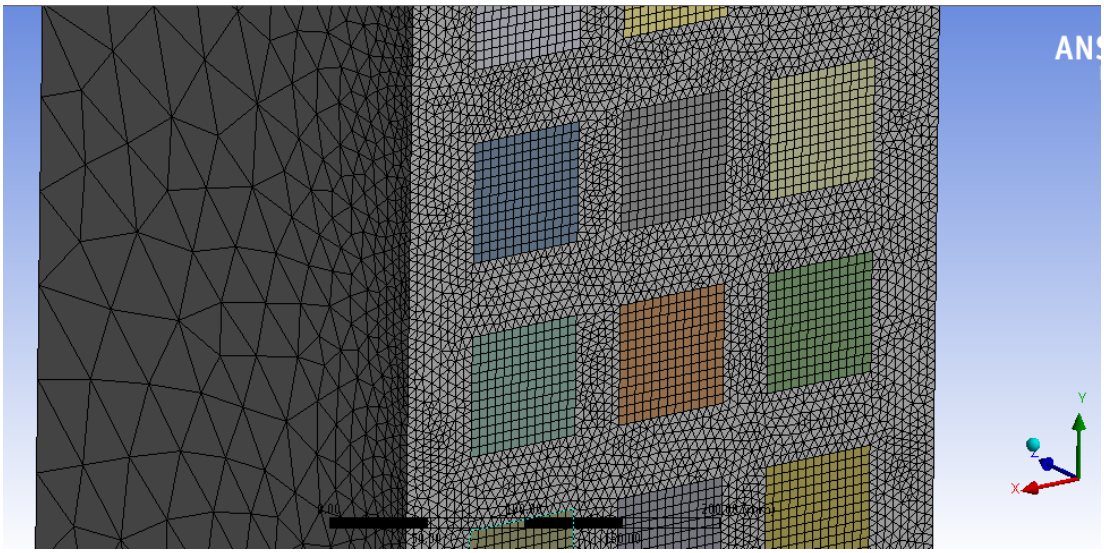

Appendix 3: Temperature along line data series (Cold air duct).

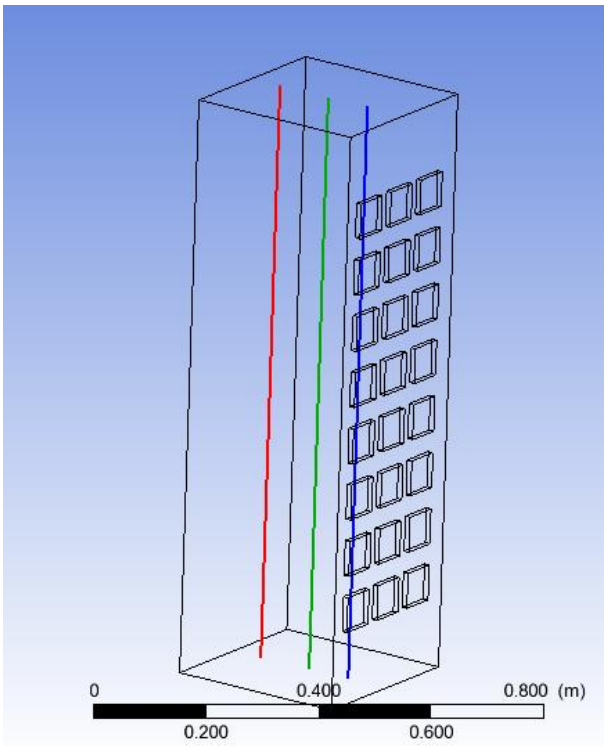

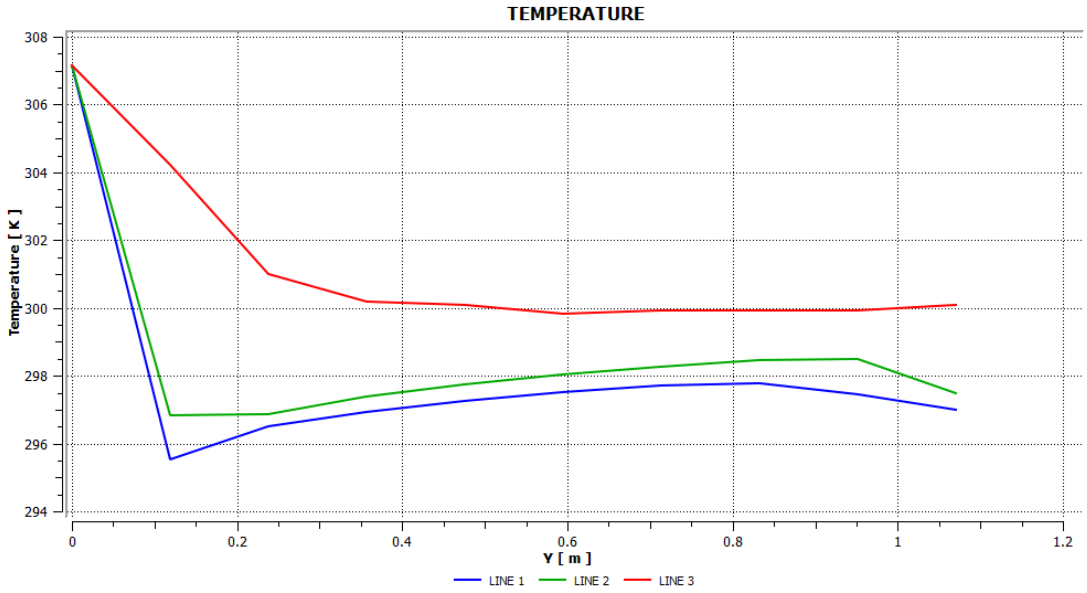

Appendix 4: Pressure along line data series (Cold air duct).

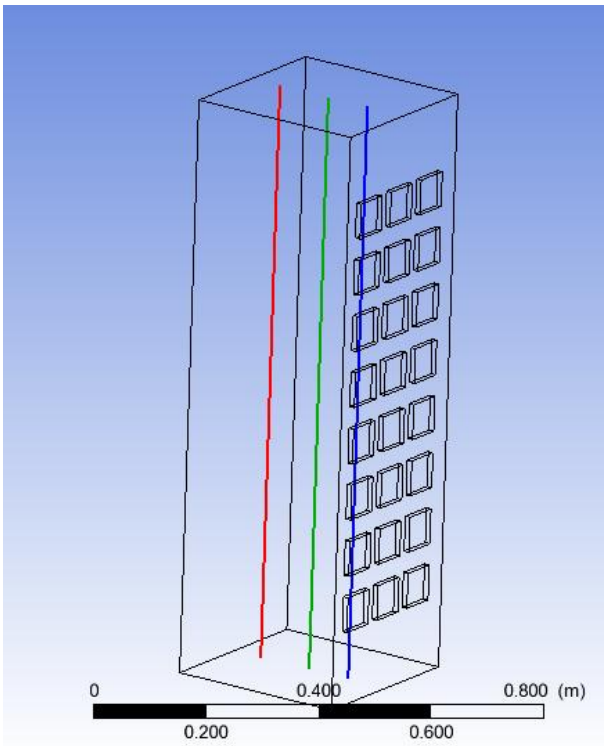

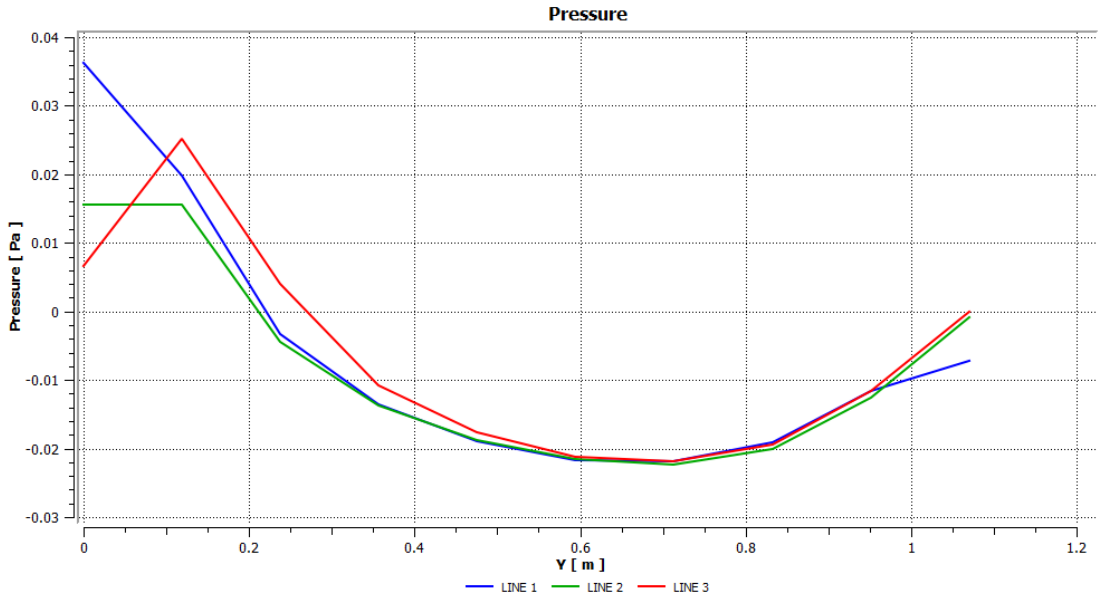

Appendix 5:Temperature Contour (Cold and Hot air duct).

Cold air Duct.

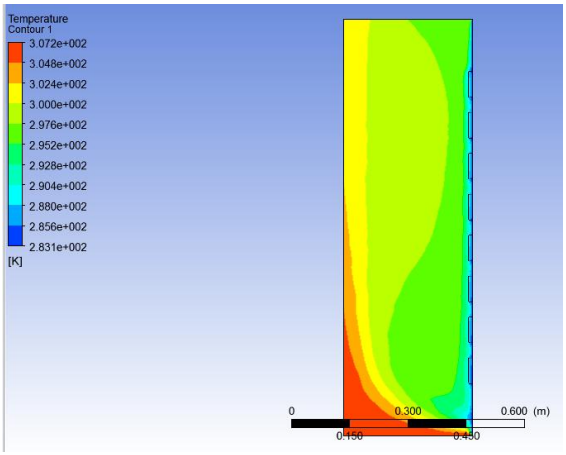

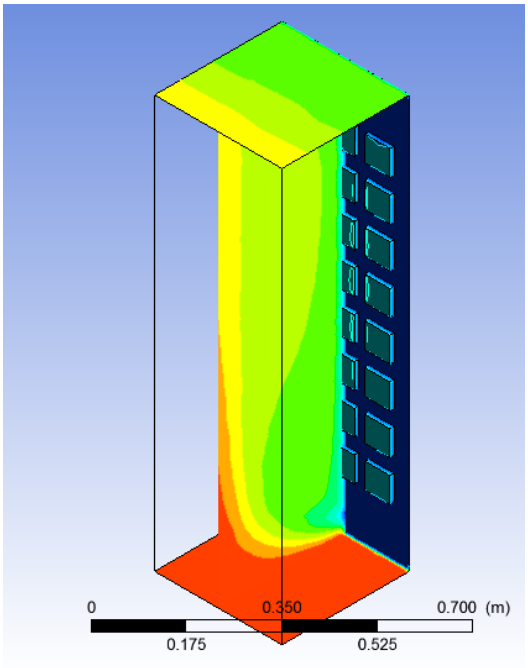

Hot Air Duct.